



Universiteit  
Leiden

The Netherlands

## Single-molecule microscopy in zebrafish embryos

Góra, R.J.

### Citation

Góra, R. J. (2022, November 23). *Single-molecule microscopy in zebrafish embryos*. Retrieved from <https://hdl.handle.net/1887/3487015>

Version: Publisher's Version

License: [Licence agreement concerning inclusion of doctoral thesis in the Institutional Repository of the University of Leiden](#)

Downloaded from: <https://hdl.handle.net/1887/3487015>

**Note:** To cite this publication please use the final published version (if applicable).

## 5. SUMMARY AND DISCUSSION

### 5.1 SUMMARY OF THE THESIS

Single-molecule microscopy (SMM) techniques constitute potent tools that facilitate the imaging of individual particles over time. With help of these techniques, it is possible to analyze the dynamics of single molecules in a variety of biological systems and to study the impact of structural and biochemical components on their mobility patterns. In this thesis, we have optimized three advanced fluorescence microscopy techniques and applied them to perform SMM in the zebrafish embryo model. We have used two proteins to investigate the consistency and reproducibility of the results obtained using our *in vivo* SMM approaches: H-Ras as a model membrane protein and the glucocorticoid receptor (GR) as a model nuclear protein.

In **Chapter 2** of this thesis, we have investigated the mobility patterns of the full-length functional H-Ras protein in the epidermal apical membranes of living two-day-old zebrafish embryos using TIRF microscopy. We found that in these cells H-Ras is present in two distinctive fractions, one that is fast-diffusing and another that is slow-diffusing. Interestingly, we discovered that both H-Ras fractions do not diffuse freely throughout the entire surface of the plasma membrane, but that they show confinement to specific membrane microdomains. By studying a constitutively active mutant H-Ras protein, we demonstrated that the activation status of the H-Ras protein plays a role in defining its dynamics. In particular, the diffusion coefficient and the confinement area of the fast-diffusing fraction were increased compared to the wild type H-Ras protein. Subsequently, to determine the nature of the membrane microdomains that form the confinement zones, we tested whether these zones represented so-called lipid rafts, which are dependent on the presence of cholesterol and the actin filaments attached to the plasma membrane. We found that cholesterol depletion and disruption of the actin cytoskeleton had a similar effect on the H-Ras mobility, also increasing the diffusion coefficient and the confinement area of the fast-diffusing fraction, suggesting that the fast-diffusing fraction of the inactive form of H-Ras resides in lipid rafts, whereas for the active form this fraction is predominantly located in larger, cholesterol- and actin-independent domains. Furthermore, by analyzing the sources variability of the data, we

demonstrated that the differences between individual cells within a tissue, rather than differences between embryos, were the main contributors to the variation in our results.

Following the TIRFM studies performed on H-Ras *in vivo*, in **Chapter 3** we employed multifocal 2PEF microscopy, which significantly reduces out-of-focus phototoxicity to the biological samples along with the photobleaching of the fluorophores. By the use of this technology, we succeeded in visualizing H-Ras anchor molecules over longer periods, which enabled us to reconstruct their trajectories. This way, we departed from the population-based description of the single-molecule dynamics and focused on analyzing molecular trajectories of individual H-Ras anchor molecules. We used this approach to analyze the mobility pattern of the H-Ras membrane anchor fused to GFP in the membranes of epidermal cells of zebrafish embryos. This imaging approach enabled us to solely detect the slow-diffusing population of molecules and perform a detailed analysis of their dynamic behavior. The analysis of the trajectories revealed that the GFP-tagged H-Ras anchors of the slow-diffusing subpopulation continuously switch between a diffusing and a hopping mode. Strikingly, we found that the time they spend in the hopping state is relatively short compared to the time spent in the diffusing state, implying that the anchors exhibit an anomalous mode of diffusion, which could be referred to as molecular hopping.

Finally, in **Chapter 4** of this thesis, we aimed to test whether it is also possible to perform SMM beyond the membranes of the zebrafish epidermal cells. To this end, we employed LSF microscopy that creates a plane of light, called a light sheet, which only excites the fluorophores present in the illuminated plane. For long-term imaging of the zebrafish embryos using this microscopy technique, we designed a custom-made imaging chamber. With the customized LSF microscopy setup in place, we visualized single glucocorticoid receptors (GRs) inside the yolk syncytial nuclei (YSN) of one-day-old embryos, and analyzed their mobility patterns. As previously found in cultured cells, we identified a fast- and a slow-diffusing population of GRs in our *in vivo* system. By treating the embryos with the GR agonist, dexamethasone, we decreased the diffusion of the GRs, confirming results previously found in cultured cells and thereby validating the *in vivo* measurements. Similarly to the H-Ras data, most of the variability in the results came from imaging different cells within an individual zebrafish embryo.

## 5.2 THE MOBILITY PATTERNS OF H-RAS AND C10H-RAS IN EPIDERMAL CELLS OF LIVING ZEBRAFISH EMBRYOS (*Chapters 2 and 3*)

To analyze the mobility patterns of H-Ras, H-Ras mutants and C10H-Ras molecules in the membranes of epidermal cells in zebrafish embryos in detail, we utilized two different SMM techniques. By using TIRF microscopy, we were able to image individual proteins with a temporal resolution of 25 ms, which enabled us to determine the existence of two H-Ras subpopulations with different diffusion coefficients and the size of their confinement area. As the photobleaching in the TIRF illumination significantly affects the lifespan of the fluorescent molecules, it is impractical to reconstruct the tracks of molecules over more than a few image frames for the vast majority of molecules. Hence, to bypass this issue, we employed a 2PEF microscopy technique that, due to its two-photon excitation mode, allowed us to limit photobleaching and increase the lifetime of the fluorophores genetically fused to the H-Ras anchors and, consequently, properly reconstruct their trajectories.

Throughout the first investigations of the H-Ras mobility patterns in which we used TIRF microscopy, we observed that the H-Ras proteins are present in two distinctive subpopulations, a fast- and a slow-diffusing one, which both showed confined diffusion. The presence of the two subpopulations was consistent and reproducible between different experimental approaches that we employed, i.e., between experiments performed in HEK293T cells and the ones performed in epidermal cells of zebrafish embryos, between different developmental stages of the zebrafish embryos, and between the full-length, functional H-Ras protein and its membrane anchor, C10H-Ras, as well as its constitutively active (H-Ras<sup>V12</sup>) and inactive (H-Ras<sup>N17</sup>) mutants. The existence of different dynamic subpopulations validated our *in vivo* experimental approach, as the fast- and slow-diffusing fractions had already been observed in several single-molecule studies conducted in cultured cells on full-width H-Ras (Lommerse et al., 2005; Lommerse et al., 2006) and on its anchoring domain C10H-Ras, which had also been studied in zebrafish embryos (Lommerse et al., 2004; Schaaf et al., 2009).

During our investigations, we noticed that the full-length H-Ras protein traversed plasma membranes of zebrafish epidermal cells with a lower diffusion coefficient than

it did in the membranes of the HEK293T cells. This phenomenon held for both fractions of the functional H-Ras protein, however, we did not observe similar behavior in the case of C10H-Ras which showed slower diffusion in both systems. This suggested that interactions between the functional full-width H-Ras protein and cell-specific components inside the plasma membrane or cytoplasm are also involved in determining its mobility patterns. This hypothesis was strengthened by the fact that fast-diffusing fractions of H-Ras and its anchor were all confined to specific areas of the plasma membrane, which has not been reported in all previous studies (Lommerse et al., 2006; Schaaf et al., 2009). We speculate that the lack of confinement of the fast-diffusing subpopulation in earlier studies stems from the combined effects of short time ranges used (< 50 ms) and larger variability due to smaller sample sizes.

In the next set of experiments, we evaluated the role of H-Ras activation on its mobility patterns by using constitutively active and inactive H-Ras mutants, H-Ras<sup>V12</sup> and H-Ras<sup>N17</sup>, respectively. We compared the dynamic parameters determined for the wild-type H-Ras protein and its C10H-Ras to the parameters obtained for H-Ras<sup>V12</sup> and H-Ras<sup>N17</sup>. We found that the constitutively active mutant H-Ras<sup>V12</sup> displayed a significantly larger diffusion coefficient and size of its confinement area for the fast-diffusing subpopulation in comparison to the same population of wild-type H-Ras, C10H-Ras, and H-Ras<sup>N17</sup> proteins. As the other three H-Ras constructs (H-Ras, C10H-Ras, and H-Ras<sup>N17</sup>) exhibited similar mobility patterns, distinct from the H-Ras<sup>V12</sup> pattern, we concluded that the vast majority of the wild-type H-Ras proteins diffusing in the epidermal cells of zebrafish embryos are in an inactive state. Because it had also been shown that H-Ras<sup>V12</sup> can induce oncogenic changes in a variety of zebrafish cell types upon overexpression, we conclude that the altered mobility is associated with the active signaling of this protein in the zebrafish cells (Feng et al., 2010; Michailidou et al., 2009; Santoriello et al., 2010).

The increased mobility of the active mutant H-Ras<sup>V12</sup> probably originated from an altered affinity of H-Ras proteins for specific plasma membrane microdomains upon activation, which has been demonstrated before (Hancock and Parton, 2005; Plowman et al., 2005; Prior et al., 2001; Prior et al., 2003; Zhou et al., 2018). A myriad of scientific reports has revealed that the H-Ras and its anchor alone both can form nanoclusters that are located in small lipid rafts (Fig. 1) (Plowman et al., 2005; Prior et al., 2001; Prior et al., 2003). These lipid rafts are domains of 10-100 nm in size that are dependent on the presence

of cholesterol (Garcia-Parajo et al., 2014; Lingwood and Simons, 2010; Nickels et al., 2015; Zhou and Hancock, 2015). Interestingly, a similar dependence on cholesterol was observed for nanoclusters of activated, GTP-loaded, N-Ras, but not for K-Ras nanoclusters or active forms of H-Ras, indicating the formation of alternative nanoclusters in distinct membrane domains that appear to be slightly smaller and cholesterol-independent (Plowman et al., 2005; Prior et al., 2001; Prior et al., 2003). Such a preferential dependence on lipids suggests that each type of Ras nanoclusters has a unique lipid composition and, therefore, reflects varying lipid-binding properties between different Ras proteins and between their active and inactive forms (Zhou et al., 2018). For example, phosphatidylserine (PtdSer) and phosphatidylinositol 4-phosphate are found in clusters of both GDP- and GTP-bound H-Ras, but only K-Ras localization and clustering on the plasma membrane are sensitive to varying PtdSer concentrations, enabling PtdSer content-sensitive sorting of H- and K-Ras into spatially distinctive lipid assemblies (Zhou et al., 2014). These results show that Ras nanoclusters assemble a distinctive set of plasma membrane phospholipids, which corresponds to their specific effector activation profiles (Zhou and Hancock, 2015; Zhou et al., 2018).

Increased diffusion coefficients and confinement zone of the fast-diffusing fraction observed for H-Ras<sup>V12</sup> in our study most likely reflect the different diffusion properties of the domains to which the activated H-Ras localizes. The lower affinity for lipid rafts is associated with an increased diffusion rate and confinement zone size. These confinement zones in the plasma membrane have been suggested to underline the concept of membrane compartmentalization resulting from the structure of the membrane cytoskeleton, a filamentous actin meshwork associated with the cytoplasmic surface of the plasma membrane, and various transmembrane proteins anchored to these actin filaments (Fujiwara et al., 2002; Kusumi et al., 2010). We argue that the diffusion of non-active H-Ras clusters is even more hindered by these cytoskeleton-based boundaries than the clusters of activated H-Ras molecules, due to the size of the lipid rafts they are localized in (Fig. 1).

Subsequently, we presented that methyl- $\beta$ -cyclodextrin (MBCD) administration also increased the initial diffusion coefficients and size of confinement areas for wild-type H-Ras and H-Ras<sup>V12</sup>. In the presence of this compound, the differences between the mobility patterns of the non-activated and activated form of H-Ras were no longer

observed. MBCD leads to cholesterol depletion in the cells and, therefore, the disruption of lipid raft formation, which is in line with the largest effect of this compound on the non-active H-Ras that has a higher affinity for lipid rafts. It has been shown that LatB also disrupts the clustering of non-active H-Ras forms and, therefore, that an intact cytoskeleton is required for lipid raft formation (Plowman et al., 2005). Since it has also been shown that cholesterol depletion disrupts the actin cytoskeleton, the interaction between lipid rafts and the cytoskeleton seems to be bidirectional (Kwik et al., 2003).

In addition, previous evidence showed that GTP-loading increased the probability of H-Ras clusters being transiently ( $< 1$  s) immobilized (Murakoshi et al., 2004), and that interactions with many cytoplasmic proteins, such as Galectin-1 and Sur-8, appear to be involved in the formation of these immobile H-Ras clusters, which are considered to be the sites where active signaling occurs (Belanis et al., 2008; Hancock and Parton, 2005; Herrero et al., 2016; Li et al., 2000; Shalom-Feuerstein et al., 2008; Zhou et al., 2018). The slow-diffusing fraction observed in our study had a diffusion rate similar to this previously identified immobile population (Murakoshi et al., 2004), and we suggest that the slow-diffusing population contains the actively signaling H-Ras molecules. In addition, after fitting the three-population model, it has been possible to further subdivide the slow-diffusing fraction by distinguishing an immobile population. Contrary to the previous experiments performed in cultured cells (Lommerse et al., 2005; Murakoshi et al., 2004), the size of the slow-diffusing fraction in the current study was not increased for the active form of H-Ras. Ultimately, the size of the slow-diffusing H-Ras fraction decreased significantly for both wild-type H-Ras and H-Ras<sup>V12</sup> upon treatment with LatB and MBCD, which underlines the importance of the structure and composition of the plasma membrane in the process of H-Ras clusters immobilization.

Using multifocal 2PEF microscopy, we focused our attention on the mobility patterns of the slow-diffusing population of C10H-Ras molecules. First, we optimized the 2PEFM technique to image single molecules in living zebrafish embryos. However, with a time lag of 200 ms, it was not possible to image fluorescent molecules that belonged to the fast-diffusing fraction that we had previously identified in our TIRF microscopy studies. Nevertheless, owing to the imaging mode, the photobleaching of the fluorescent molecules was greatly reduced, which enabled us to visualize the slow-diffusing C10H-Ras molecules for a time ranging from 3 to 15 seconds and, consequently, reconstruct their

trajectories. Throughout the single-step photobleaching analysis, we were able to distinguish individual photobleaching steps, which signified that H-Ras anchor molecules in the slow-diffusing population form clusters consisting of varying numbers of molecules. Following that, we uncovered that single H-Ras membrane anchor mobility patterns are more suitably presented by the analysis of their trajectories rather than by the population-based examination of the mean squared displacements. The C10H-Ras molecules appeared to switch between two different states, a diffusing and a hopping one (Fig. 1). For most of the time, these molecules resided in a diffusing state and this diffusion was interrupted by brief periods of hopping. The total time spent in this hopping state was approximately four to five times shorter than the C10H-Ras molecules spend in the diffusing state, and the ratio between the time spent in the hopping state and the diffusion state equaled 0.237. Taken together, our findings revealed that the H-Ras membrane anchors exhibit an anomalous mobility pattern, which can be referred to as molecular hopping.

The events of molecular hopping for the H-Ras membrane anchor or the full-length H-Ras protein had not been observed before. However, it has been reported that many signaling proteins experience two-dimensional hop diffusion on the membrane in search of their target and because of the packed structure of the plasma membrane itself (Campagnola et al., 2015; Umemura et al., 2008; Yasui et al., 2014). The plasma membrane is made of hundreds of microdomains, caused by the actin-based membrane skeleton, which is closely associated with the cytoplasmic surface of the plasma membrane. Consequently, many transmembrane proteins collide with the membrane skeleton, which induces temporary confinement of the transmembrane proteins in the membrane-skeleton meshwork. Thus, in the vicinity of immobilized molecules located in the membrane, the movement of any other particles is extremely limited. With all these obstacles, membrane proteins often hop from one microdomain to another one, especially when thermal fluctuations of the membrane and the actin meshwork associated with it create sufficient space between them to enable the passage of integral membrane proteins, or when an actin filament is temporarily severed (Suzuki et al., 2005)



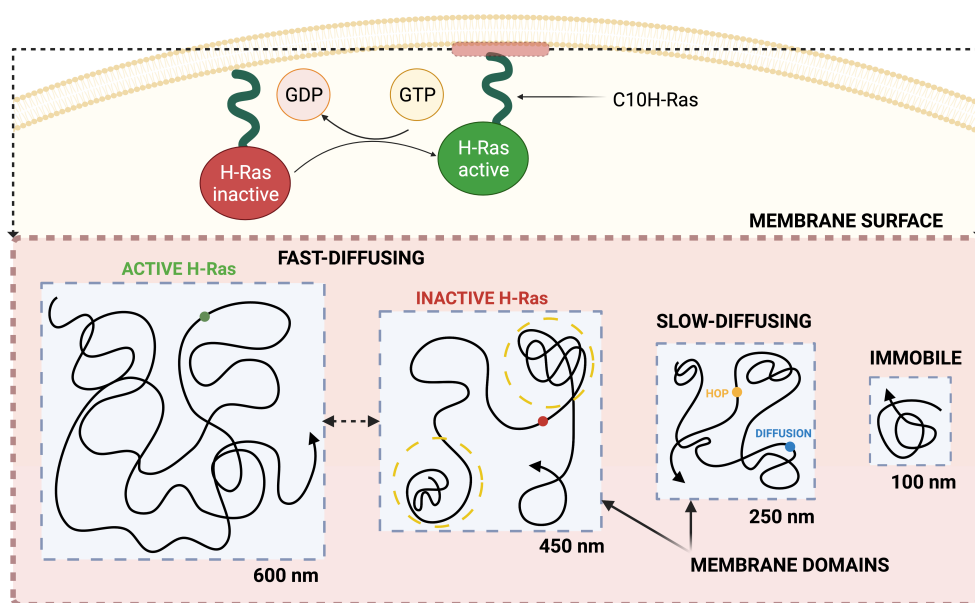


**FIGURE 1: Summary of the H-Ras anchor mobility patterns in the membranes of epidermal cells in the living zebrafish embryos.** Analysis of the TIRFM data revealed the presence of two dynamic subpopulations of Ras proteins, a fast- and a slow-diffusing one. The data from 2PEFM allowed for further addition of an immobile subpopulation, in which particles barely diffused. In the fast-diffusing fraction, inactive, GDP-loaded H-Ras mostly resides in lipid rafts which limits its mobility, confining it to an area that is smaller than the cholesterol-independent area in which the active, GTP-loaded H-Ras, is predominantly diffusing. This confinement most likely results from transmembrane proteins, lipids, and the actin meshwork attached to the plasma membrane. In the slow-diffusing fraction, it has been possible, using the 2PEFM results, to distinguish two different states in which the H-Ras molecules can occur: a diffusing and a hopping state. This hopping state is relatively sporadic and brief, occurring approximately four times less frequent than the diffusing state.

Such a temporary nature of protein-membrane interactions enables a tight temporal regulation of signal transduction processes. It has also been suggested that molecular hopping might be critical in the search for target molecules in eukaryotic cells. A straightforward consequence of membrane hopping is that a molecule remains in its immediate vicinity for a short time and then jumps to a location that is further away than expected from two-dimensional diffusion. In such a way, the search process is allowed to explore larger areas, which allows proteins to bypass diffusion barriers that may be present in the membrane (Lemmon, 2008). Since the H-Ras membrane anchor experiences this type of diffusion, we suggest that this process is governed

predominantly by electrostatic, membrane-protein associations, and not by interaction with other proteins and does not involve active protein signaling.

### **5.3 THE MOBILITY PATTERN OF THE GLUCOCORTICOID RECEPTOR IN LIVING ZEBRAFISH EMBRYOS (*Chapter 4*)**

We used LSF microscopy to enable the analysis of the dynamics of intracellular proteins in living zebrafish embryos, and we used this approach to study the mobility patterns of GR inside the yolk syncytial nuclei (YSN). This analysis revealed that the GRs in the YSN are divided into a fast- and a slow-diffusing subpopulation. The existence of two fractions had been observed before for GR and other transcription factors. The fast and the slow fraction are generally considered to reflect GRs that diffuse freely within the nucleus, and receptors that interact with DNA, respectively. In a recent study, it was shown that the fast subpopulation could, in turn, be divided into two fractions with different mobility, of which the fastest one was interpreted as receptors diffusing freely through the nucleus, and the slowest one as GRs interacting non-specifically with the DNA (Keizer et al., 2019).

Our findings show that the vast majority of the GR molecules in the YSN belonged to the fast subpopulation, which constituted around 90% of the total GR population in the vehicle-, and 77% in the dexamethasone-treated group. This percentage is significantly higher than previously observed in cultured cells, where this fraction was estimated to constitute between 45 and 60% of the total number of molecules diffusing in the nuclei upon activation by either cortisol or dexamethasone (Alsop and Vijayan, 2009; Groeneweg et al., 2014; Keizer et al., 2019). The difference between our control-treated zebrafish embryos and previously reported cortisol-treated cellular models can be explained by a lack of a properly developed cortisol secretion in two-day-old embryos (Alsop and Vijayan, 2009), but this does not account for the differences between these models upon dexamethasone treatment. The high percentage of fast-diffusing molecules is better explained by the large size of the YSN, between 8 and 12  $\mu\text{m}$ . A larger fraction of freely-diffusing GRs may be expected with more space available in the YSN and the same amount of chromatin present. GR molecules in either of the subpopulations did not move within the entire nuclear environment, but were confined to areas with a size of around 1233 nm for the fast subpopulation and 322 nm for the slow

subpopulation. The confinement of the GRs has not been observed in previous studies on the receptor mobility patterns. In our approach, however, we were able to reconstruct the squared displacements of GRs in both fractions over a longer time, which enabled us to determine the occurrence of nuclear areas in which the diffusion of the GRs is restricted. Such confinement of the fast GR subpopulation indicates that the receptors diffuse within areas surrounded by barriers, which in the nucleus could be formed by chromatin. In addition to that, previous studies reported values for the diffusion coefficients of the GR fast fraction to be within the range of circa 2.5 and 9  $\mu\text{m}^2 \text{s}^{-1}$  (Gebhardt et al., 2013; Groeneweg et al., 2014; Keizer et al., 2019), and similar values have been observed for other transcription factors, such as p53 or STAT1 (Mazza et al., 2012; Speil et al., 2011). The values for the diffusion coefficient of the fast subpopulation that were obtained in our approach, i.e.,  $7.90 \pm 0.53 \mu\text{m}^2 \text{s}^{-1}$ , fall well within the previously published range. The slow subpopulation was characterized by a tenfold lower diffusion coefficient ( $0.78 \pm 0.18 \mu\text{m}^2 \text{s}^{-1}$ ), which agreed with the values reported previously, estimated to range between 0.03 and 0.50  $\mu\text{m}^2 \text{s}^{-1}$  (Gebhardt et al., 2013; Groeneweg et al., 2014; Keizer et al., 2019).

In the next step of this study, we found that treating zebrafish embryos with dexamethasone did not significantly alter the size of the fast-diffusing fraction of GRs. In previous studies, it had consistently been shown that administration of a GR agonist decreased the size of the fast subpopulation, believed to reflect a larger fraction of GRs that interact with the DNA to modulate the transcription of genes (Groeneweg et al., 2014). The lack of a dexamethasone effect on the population size in our study might, therefore, be specific to the zebrafish GR, or the specific cell type studied. Despite the lack of effect on the size of the fast subpopulation, incubation of the embryos with dexamethasone did result in a significant decrease of the diffusion coefficients both for the fast- and the slow-diffusing fraction. Lower diffusion coefficients of the fast-diffusing GRs most likely reflect non-specific binding events to DNA in search of their proper binding site, which slow down their diffusion rate (Keizer et al., 2019). Additionally, treatment with dexamethasone reduced the size of the confinement area for the fast-diffusing subpopulation of GRs. This can be explained by the dexamethasone-activated GR molecules constituting a part of larger multi-protein complexes. These complexes, made of receptor molecules and transcriptional coregulatory proteins, are present inside the cell nuclei and take part in the transcription of GR target genes. Diffusion of the

GR molecules in these bulky multi-protein aggregates might, thus, be hindered, resulting in the smaller confinement areas in the dexamethasone-treated groups. Our results, therefore, are in accordance with previous findings that indicated that the interactions between ligand and receptor determine the binding events between the GR and the DNA inside the nucleus.

#### **5.4 THE SOURCES OF VARIABILITY OF THE SMM MEASUREMENTS IN THE ZEBRAFISH EMBRYO MODEL (*Chapters 2 and 4*)**

In addition to analyzing the mobility patterns of H-Ras and GR, we have assessed and characterized the variability of the dynamic parameters that we had determined in our zebrafish embryo model. For this purpose, we specified the factors that contributed the most to the variability present in the mobility data obtained during our investigations. Surprisingly, differences between individual embryos had only a modest effect on the overall variation in the results of the H-Ras studies. However, different areas of the embryonic epidermis and different experimental days both appeared to be factors that have largely contributed to the variation in the data. This indicates that the differences between cells within the epidermal tissue of one individual embryo are larger than the differences observed between embryos, and suggests that the cellular context is the main determinant of H-Ras mobility.

In the GR study, the existing variability mostly originated from imaging different cell areas within an individual embryo, too, and this variability was most prominent in the measured mobility patterns exhibited by the fast subpopulation of GRs. We, therefore, suggest that it is the architecture of the nucleus, in particular a specific organization of the nuclear chromatin, that likely affected the diffusion behavior of the fast-diffusing GRs. Additionally, variability was observed between the dynamic parameters displayed by individual zebrafish embryos, and this variability might have originated from genetic variation between different zebrafish batches. The absence of inbred zebrafish strains causes this inherent genetic variability and could have been a factor that contributed to the overall variability of the parameters describing the GR mobility patterns. This source of variation might in the future be avoided by utilizing embryos from one selected couple of adult zebrafish per experiment.

## 5.5 FUTURE PERSPECTIVES

Taken together, this thesis extends the applications of the SMM techniques to study the mobility patterns of single membrane and nuclear proteins *in vivo*. Whereas the thesis provides the foundations for imaging the living vertebrate organisms using a variety of SMM techniques, there are several aspects that, if properly implemented, will most certainly improve the quality of the obtained single-molecule data. These aspects include better protein labelling technology, the development of three-dimensional single-molecule imaging methods, and the improvement of the temporal resolution of the SMM setups. In **Chapter 2** we present that, while being a useful starting point for imaging single molecules *in vivo*, traditional autofluorescent proteins suffer from photobleaching and are not optimal for long-term measurement protocols. It is inherent to the TIRF microscopy technique that it is limited to visualization of structures localized in the vicinity of the coverglass-sample interface, making it impossible to image molecules located deeper in the epidermis of the zebrafish embryo model. The use of organic dyes, commonly applied to Halo- and SNAP-tags has thus far been optimized only for *in vitro* SMM studies. Extension of their application to more complex, biological models would enable the use of superior fluorophores with a higher photostability and quantum yield, which are excitable by a different wavelength of light, enabling the use of wavelengths that cause significantly reduced autofluorescence of these biological samples, and thereby improve the SNR of the acquired images. Following that, in **Chapter 3**, we show that reduced out-of-focus photobleaching enables following single molecules over longer times than in experiments in which TIRFM and LSFM techniques are used. Yet, we point to the fact that insufficient temporal resolution of the microscopy setup leads to blurring effects that result in missing the fastest molecules in the population. An improvement of the quantum yield of the microscopy setup detector (Mondal, 2014) and, therefore, an increase in the temporal resolution of the setup, is critical for a better imaging output. Lastly, in **Chapter 4**, we provide the evidence that many molecules do not move along the membranes, but rather inside entire organelles, i.e., in three dimensions. The possibilities of the SMM techniques being performed in three dimensions *in vivo* are limited and often compromise other imaging parameters, such as temporal or spatial resolution. Currently, the lack of information about mobility in the third dimension is often compensated by computational simulations and stochastic models,

including the Markov chain model. Nonetheless, a few successful studies on *in vitro* 3D imaging of single molecules, such as the transcription factor Sox2, have already been performed (Chen et al., 2014; Liu et al., 2014). Hence, SMM imaging *in vivo* in three dimensions together with other, previously mentioned aspects, all indicate some of the most urgent directions that the future development of SMM imaging *in vivo* should follow.

## REFERENCES

- Alsop, D. and Vijayan, M. M.** (2009). Molecular programming of the corticosteroid stress axis during zebrafish development. *Comp. Biochem. Physiol. A. Mol. Integr. Physiol.* **153**, 49–54.
- Belanis, L., Plowman, S. J., Rotblat, B., Hancock, J. F. and Kloog, Y.** (2008). Galectin-1 is a novel structural component and a major regulator of h-ras nanoclusters. *Mol. Biol. Cell* **19**, 1404–1414.
- Campagnola, G., Nepal, K., Schroder, B. W., Peersen, O. B. and Krapf, D.** (2015). Superdiffusive motion of membrane-targeting C2 domains. *Sci. Rep.* **5**, 17721.
- Chen, J., Zhang, Z., Li, L., Chen, B.-C., Revyakin, A., Hajj, B., Legant, W., Dahan, M., Lionnet, T., Betzig, E., et al.** (2014). Single-molecule dynamics of enhanceosome assembly in embryonic stem cells. *Cell* **156**, 1274–1285.
- Feng, Y., Santoriello, C., Mione, M., Hurlstone, A. and Martin, P.** (2010). Live imaging of innate immune cell sensing of transformed cells in zebrafish larvae: parallels between tumor initiation and wound inflammation. *PLoS Biol.* **8**, e1000562.
- Fujiwara, T., Ritchie, K., Murakoshi, H., Jacobson, K. and Kusumi, A.** (2002). Phospholipids undergo hop diffusion in compartmentalized cell membrane. *J. Cell Biol.* **157**, 1071–1081.
- Garcia-Parajo, M. F., Cambi, A., Torreno-Pina, J. A., Thompson, N. and Jacobson, K.** (2014). Nanoclustering as a dominant feature of plasma membrane organization. *J. Cell Sci.* **127**, 4995–5005.
- Gebhardt, J. C. M., Suter, D. M., Roy, R., Zhao, Z. W., Chapman, A. R., Basu, S., Maniatis, T. and Xie, X. S.** (2013). Single-molecule imaging of transcription factor binding to DNA in live mammalian cells. *Nat. Methods* **10**, 421–426.
- Groeneweg, F. L., Royen, M. E. van, Fenz, S., Keizer, V. I. P., Geverts, B., Prins, J., Kloet, E. R. de, Houtsmuller, A. B., Schmidt, T. S. and Schaaf, M. J. M.** (2014). Quantitation of Glucocorticoid Receptor DNA-Binding Dynamics by Single-Molecule Microscopy and FRAP. *PLOS ONE* **9**, e90532.
- Hancock, J. F. and Parton, R. G.** (2005). Ras plasma membrane signaling platforms. *Biochem. J.* **389**, 1–11.
- Herrero, A., Matallanas, D. and Kolch, W.** (2016). The spatiotemporal regulation of RAS signaling. *Biochem. Soc. Trans.* **44**, 1517–1522.
- Keizer, V. I. P., Coppola, S., Houtsmuller, A. B., Geverts, B., van Royen, M. E., Schmidt, T. and Schaaf, M. J. M.** (2019). Repetitive switching between DNA-binding modes enables target finding by the glucocorticoid receptor. *J. Cell Sci.* **132**, jcs217455.

- Kusumi, A., Shirai, Y. M., Koyama-Honda, I., Suzuki, K. G. N. and Fujiwara, T. K.** (2010). Hierarchical organization of the plasma membrane: investigations by single-molecule tracking vs. fluorescence correlation spectroscopy. *FEBS Lett.* **584**, 1814–1823.
- Kwik, J., Boyle, S., Fooksman, D., Margolis, L., Sheetz, M. P. and Edidin, M.** (2003). Membrane cholesterol, lateral mobility, and the phosphatidylinositol 4,5-bisphosphate-dependent organization of cell actin. *Proc. Natl. Acad. Sci. U. S. A.* **100**, 13964–13969.
- Lemmon, M. A.** (2008). Membrane recognition by phospholipid-binding domains. *Nat. Rev. Mol. Cell Biol.* **9**, 99–111.
- Li, W., Han, M. and Guan, K. L.** (2000). The leucine-rich repeat protein SUR-8 enhances MAP kinase activation and forms a complex with Ras and Raf. *Genes Dev.* **14**, 895–900.
- Lingwood, D. and Simons, K.** (2010). Lipid Rafts As a Membrane-Organizing Principle. *Science* **327**, 46–50.
- Liu, Z., Legant, W. R., Chen, B.-C., Li, L., Grimm, J. B., Lavis, L. D., Betzig, E. and Tjian, R.** (2014). 3D imaging of Sox2 enhancer clusters in embryonic stem cells. *eLife* **3**, e04236–e04236.
- Lommerse, P. H. M., Blab, G. A., Cognet, L., Harms, G. S., Snaar-Jagalska, B. E., Spaink, H. P. and Schmidt, T.** (2004). Single-Molecule Imaging of the H-Ras Membrane-Anchor Reveals Domains in the Cytoplasmic Leaflet of the Cell Membrane. *Biophys. J.* **86**, 609–616.
- Lommerse, P. H. M., Snaar-Jagalska, B. E., Spaink, H. P. and Schmidt, T.** (2005). Single-molecule diffusion measurements of H-Ras at the plasma membrane of live cells reveal microdomain localization upon activation. *J. Cell Sci.* **118**, 1799–1809.
- Lommerse, P. H. M., Vastenhoud, K., Pirinen, N. J., Magee, A. I., Spaink, H. P. and Schmidt, T.** (2006). Single-Molecule Diffusion Reveals Similar Mobility for the Lck, H-Ras, and K-Ras Membrane Anchors. *Biophys. J.* **91**, 1090–1097.
- Mazza, D., Abernathy, A., Golob, N., Morisaki, T. and McNally, J. G.** (2012). A benchmark for chromatin binding measurements in live cells. *Nucleic Acids Res.* **40**, e119–e119.
- Michailidou, C., Jones, M., Walker, P., Kamarashev, J., Kelly, A. and Hurlstone, A. F. L.** (2009). Dissecting the roles of Raf- and PI3K-signaling pathways in melanoma formation and progression in a zebrafish model. *Dis. Model. Mech.* **2**, 399–411.
- Mondal, P. P.** (2014). Temporal resolution in fluorescence imaging. *Front. Mol. Biosci.* **1**, 11.



- Murakoshi, H., Iino, R., Kobayashi, T., Fujiwara, T., Ohshima, C., Yoshimura, A. and Kusumi, A.** (2004). Single-molecule imaging analysis of Ras activation in living cells. *Proc. Natl. Acad. Sci.* **101**, 7317–7322.
- Nickels, J. D., Smith, J. C. and Cheng, X.** (2015). Lateral organization, bilayer asymmetry, and inter-leaflet coupling of biological membranes. *Chem. Phys. Lipids* **192**, 87–99.
- Plowman, S. J., Muncke, C., Parton, R. G. and Hancock, J. F.** (2005). H-ras, K-ras, and inner plasma membrane raft proteins operate in nanoclusters with differential dependence on the actin cytoskeleton. *Proc. Natl. Acad. Sci.* **102**, 15500–15505.
- Prior, I. A., Harding, A., Yan, J., Sluimer, J., Parton, R. G. and Hancock, J. F.** (2001). GTP-dependent segregation of H-ras from lipid rafts is required for biological activity. *Nat. Cell Biol.* **3**, 368–375.
- Prior, I. A., Muncke, C., Parton, R. G. and Hancock, J. F.** (2003). Direct visualization of Ras proteins in spatially distinct cell surface microdomains. *J. Cell Biol.* **160**, 165–170.
- Santoriello, C., Gennaro, E., Anelli, V., Distel, M., Kelly, A., Köster, R. W., Hurlstone, A. and Mione, M.** (2010). Kita driven expression of oncogenic HRAS leads to early onset and highly penetrant melanoma in zebrafish. *PLoS One* **5**, e15170.
- Schaaf, M. J. M., Koopmans, W. J. A., Meckel, T., van Noort, J., Snaar-Jagalska, B. E., Schmidt, T. S. and Spaik, H. P.** (2009). Single-Molecule Microscopy Reveals Membrane Microdomain Organization of Cells in a Living Vertebrate. *Biophys. J.* **97**, 1206–1214.
- Shalom-Feuerstein, R., Plowman, S. J., Rotblat, B., Ariotti, N., Tian, T., Hancock, J. F. and Kloog, Y.** (2008). K-ras nanoclustering is subverted by overexpression of the scaffold protein galectin-3. *Cancer Res.* **68**, 6608–6616.
- Speil, J., Baumgart, E., Siebrasse, J.-P., Veith, R., Vinkemeier, U. and Kubitscheck, U.** (2011). Activated STAT1 transcription factors conduct distinct saltatory movements in the cell nucleus. *Biophys. J.* **101**, 2592–2600.
- Suzuki, K., Ritchie, K., Kajikawa, E., Fujiwara, T. and Kusumi, A.** (2005). Rapid Hop Diffusion of a G-Protein-Coupled Receptor in the Plasma Membrane as Revealed by Single-Molecule Techniques. *Biophys. J.* **88**, 3659–3680.
- Umemura, Y. M., Vrljic, M., Nishimura, S. Y., Fujiwara, T. K., Suzuki, K. G. N. and Kusumi, A.** (2008). Both MHC class II and its GPI-anchored form undergo hop diffusion as observed by single-molecule tracking. *Biophys. J.* **95**, 435–450.

**Yasui, M., Matsuoka, S. and Ueda, M.** (2014). PTEN Hopping on the Cell Membrane Is Regulated via a Positively-Charged C2 Domain. *PLoS Comput. Biol.* **10**, e1003817.

**Zhou, Y. and Hancock, J. F.** (2015). Ras nanoclusters: Versatile lipid-based signaling platforms. *Biochim. Biophys. Acta* **1853**, 841–849.

**Zhou, Y., Liang, H., Rodkey, T., Ariotti, N., Parton, R. G. and Hancock, J. F.** (2014). Signal Integration by Lipid-Mediated Spatial Cross Talk between Ras Nanoclusters. *Mol. Cell. Biol.* **34**, 862–876.

**Zhou, Y., Prakash, P., Gorfe, A. A. and Hancock, J. F.** (2018). Ras and the Plasma Membrane: A Complicated Relationship. *Cold Spring Harb. Perspect. Med.* **8**, a031831.

